ACCOUNTS of chemical research

pubs.acs.org/accounts Article

DNA Origami Nanoantennas for Fluorescence Enhancement

Viktorija Glembockyte,[†] Lennart Grabenhorst,[†] Kateryna Trofymchuk,[†] and Philip Tinnefeld*

Cite This: *Acc. Chem. Res.* 2021, 54, 3338−3348 Read Online

ACCESS | Metrics & More | Article Recommendations

CONSPECTUS: The possibility to increase fluorescence by plasmonic effects in the near-field of metal nanostructures was recognized more than half a century ago. A major challenge, however, was to use this effect because placing single quantum emitters in the nanoscale plasmonic hotspot remained unsolved for a long time. This not only presents a chemical problem but also requires the nanostructure itself to be coaligned with the polarization of the excitation light. Additional difficulties arise from the complex distance dependence of fluorescence emission: in contrast to other surface-enhanced spectroscopies (such as Raman spectroscopy), the emitter should not be placed as close as possible to the metallic nanostructure but rather needs to be at an optimal distance on the order of a few nanometers to avoid undesired quenching effects.

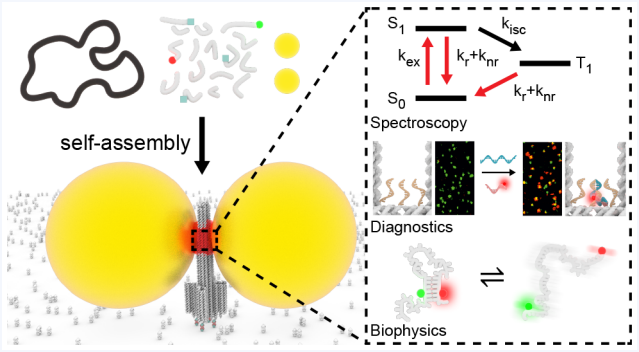

Our group addressed these challenges almost a decade ago by exploiting the unique positioning ability of DNA nanotechnology and reported the first self-assembled DNA origami nanoantennas. This Account summarizes our work spanning from this first proof-of-principle study to recent advances in utilizing DNA origami nanoantennas for single DNA molecule detection on a portable smartphone microscope.

We summarize different aspects of DNA origami nanoantennas that are essential for achieving strong fluorescence enhancement and discuss how single-molecule fluorescence studies helped us to gain a better understanding of the interplay between fluorophores and plasmonic hotspots. Practical aspects of preparing the DNA origami nanoantennas and extending their utility are also discussed.

Fluorescence enhancement in DNA origami nanoantennas is especially exciting for signal amplification in molecular diagnostic assays or in single-molecule biophysics, which could strongly benefit from higher time resolution. Additionally, biophysics can greatly profit from the ultrasmall effective detection volumes provided by DNA nanoantennas that allow single-molecule detection at drastically elevated concentrations as is required, e.g., in single-molecule DNA sequencing approaches.

Finally, we describe our most recent progress in developing DNA NanoAntennas with Cleared HOtSpots (NACHOS) that are fully compatible with biomolecular assays. The developed DNA origami nanoantennas have proven robustness and remain functional after months of storage. As an example, we demonstrated for the first time the single-molecule detection of DNA specific to antibiotic-resistant bacteria on a portable and battery-driven smartphone microscope enabled by DNA origami nanoantennas. These recent developments mark a perfect moment to summarize the principles and the synthesis of DNA origami nanoantennas and give an outlook of new exciting directions toward using different nanomaterials for the construction of nanoantennas as well as for their emerging applications.

KEY REFERENCES

- Acuna, G. P.; Möller, F. M.; Holzmeister, P.; Beater, S.; Lalkens, B.; Tinnefeld, P. Fluorescence Enhancement at Docking Sites of DNA-Directed Self-Assembled Nanoantennas. *Science* **2012**, *338*, 506−510.[1] *The first study employing the DNA origami technique to build self-assembled optical nanoantennas. The extent of fluorescence enhancement of a single dye precisely positioned in the hotspot of monomeric and dimeric nanoantennnas of nanoparticles of various sizes was studied.*
- Vietz, C.; Kaminska, I.; Sanz Paz, M.; Tinnefeld, P.; Acuna, G. P. Broadband Fluorescence Enhancement with Self-Assembled Silver Nanoparticle Optical Antennas. *ACS Nano* **2017**, *11*, 4969−4975.[2] *Fabricated DNA origami-based nanoantenna comprises large silver nanoparticles and provides fluorescent enhancement over the*

Received: May 20, 2021
Published: August 26, 2021

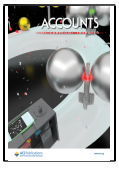

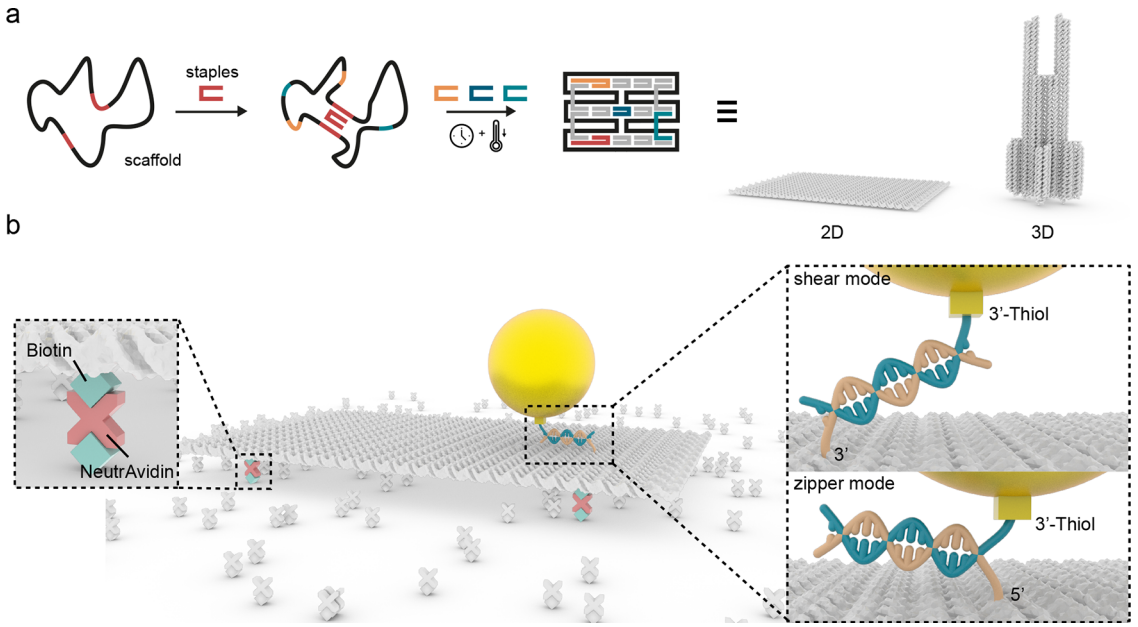

Figure 1. (a) Principle of the DNA origami approach to preparing 2D and 3D DNA nanostructures from the ssDNA scaffold and hundreds of ssDNA staple strands. (b) Immobilization of a DNA nanostructure bearing biotin-modified stands on BSA-biotin-NeutrAvidin-coated glass to perform SM fluorescence measurements (left). Attachment of ssDNA-functionalized NPs via thiol-Au/Ag interactions on DNA origami in zipper and shear binding modes, which provide different separations between DNA origami and NP (right).

visible range. A comparison between the performance of silver- and gold-based antennas is reported.

- Ochmann, S. E.; Vietz, C.; Trofymchuk, K.; Acuna, G. P.; Lalkens, B.; Tinnefeld, P. Optical Nanoantenna for Single Molecule-Based Detection of Zika Virus Nucleic Acids without Molecular Multiplication. *Anal. Chem.* **2017**, *89*, 13000−13007.[3] *Successful detection of specific DNA and RNA in heat-deactivated blood serum with the help of monomeric DNA origami antennas. Demonstration of multiplexed detection of different targets using fluorescent barcodes.*
- Trofymchuk, K.; Glembockyte, V.; Grabenhorst, L.; Steiner, F.; Vietz, C.; Close, C.; Pfeiffer, M.; Richter, L.; Schütte, M. L.; Selbach, F.; Yaadav, R.; Zähringer, J.; Wei, Q.; Ozcan, A.; Lalkens, B.; Acuna, G. P.; Tinnefeld, P. Addressable nanoantennas with cleared hotspots for single-molecule detection on a portable smartphone microscope. *Nat. Commun.* **2021**, *12*, 950.[4] *A novel design of DNA origami providing a place in the hotspot of a dimeric nanoantenna for a tailored bioassay. The first demonstration of single DNA molecule detection on a smartphone camera-based portable microscope.*

INTRODUCTION

In line with theoretical considerations by Purcell of the environment-stimulated enhancement of the emission rate of an emitter[5] and following the first experimental observations by Drexhage,[6] a whole field of research has emerged around understanding and controlling the interactions between plasmonic nanoparticles (NPs) and fluorophores. Collective oscillations of electrons in the plasmonic NPs illuminated with light at the eigenfrequency of the NPs lead to the subwavelength localization and thus enhancement of the electric field of the incident irradiation close to the surface of the NP. This property allows NPs to act as optical nanoantennas (NAs), analogous to regular radio antennas.[7,8] Key findings supported the notion of enormous potential increases in fluorescence emission rates particularly in so-called plasmonic hotspots (regions with the highest electric field enhancement)[9] while also revealing the importance of precise positioning of the fluorophore relative to the NP surface on the nanometer scale in order to avoid fluorescence quenching effects.[10]

Several approaches were employed to address this positioning problem (e.g., attaching a gold (Au) NP to the tip of an AFM cantilever,[10,11] relying on the rigidity of double-stranded DNA to couple them[12,13]); however, one method has proven particularly useful: DNA nanotechnology and, in particular, the DNA origami technique. In this approach (Figure 1a), a long (several thousands of nucleotides (nt)) single-stranded DNA (ssDNA) ("scaffold" strand) is folded in a programmable way by hybridizing with hundreds of short (∼15−50 nt) single-stranded DNA oligonucleotides ("staple" strands).[14] Specific staple strands can be modified with a molecule of interest (e.g., biotin modification or a fluorophore), and thus this molecule can be positioned on the DNA origami structure with nanometer precision. The nanoscale scaffolding capabilities of the DNA origami technique[14] are of great use when constructing the complex two- and three-dimensional (2D and 3D) geometries[15] (Figure 1a) needed to achieve high fluorescence enhancement (FE) values, and its bottom-up self-assembly reaction scheme enables the parallel production of billions of identical nanostructures. This is in sharp contrast to top-down assembly methods such as electron-beam lithography[16] which intrinsically rely on serial fabrication and only stochastic positioning of fluorescent emitters.

This Account focuses on the progress made in our group from the first DNA origami structures bearing single AuNPs toward DNA origami NanoAntennas with Cleared HOtSpots (NACHOS) that can be tailored for placing complex biomolecular assays and their potential uses in molecular

https://doi.org/10.1021/acs.accounts.1c00307
Acc. Chem. Res. 2021, 54, 3338−3348

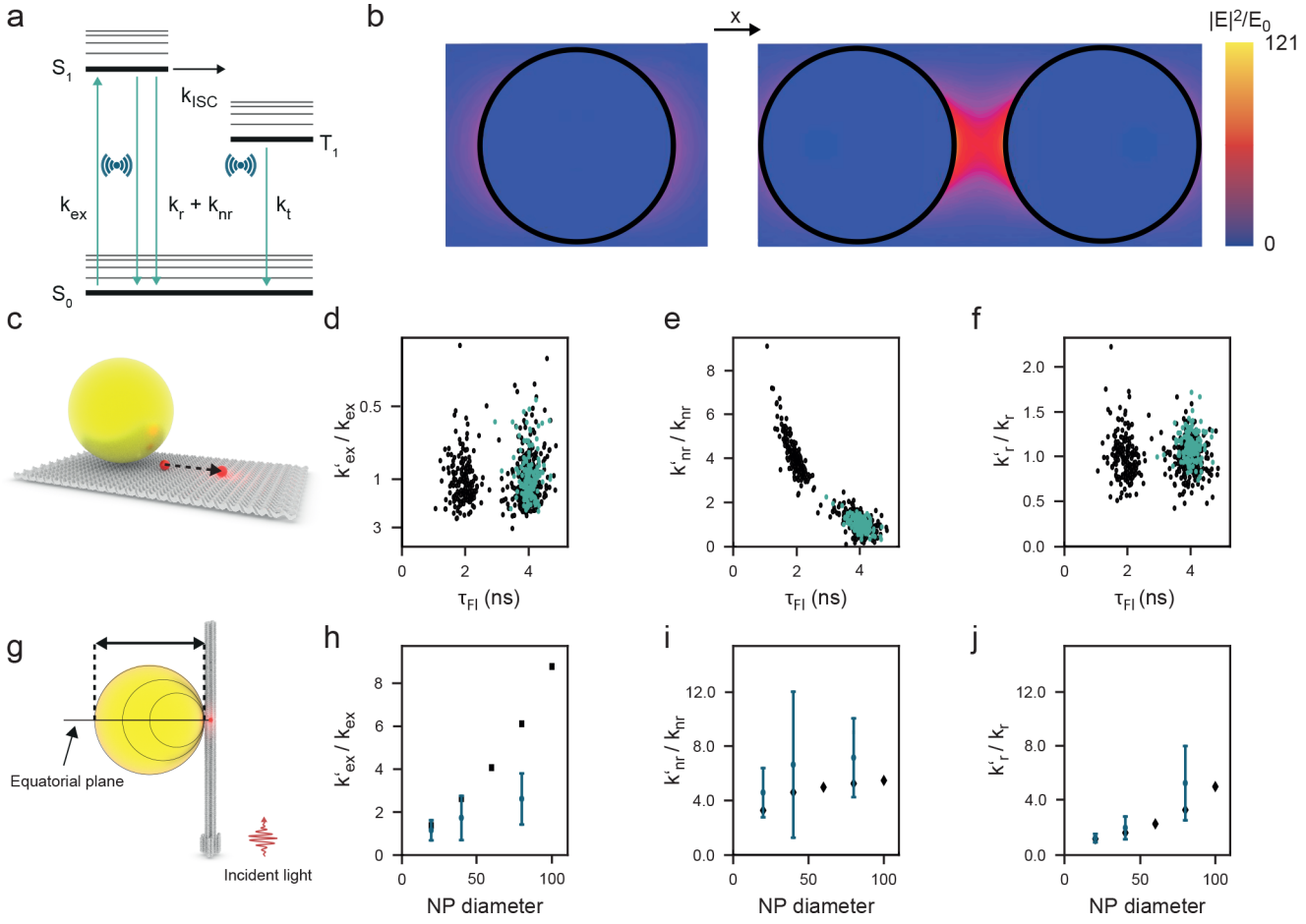

Figure 2. (a) Simplified Jablonski diagram of a fluorophore illustrating the electronic states (S_0, S_1, T_1) and the transitions between them by excitation (k_{ex}), radiative (k_r) and nonradiative (k_{nr}) decays, intersystem crossing (k_{ISC}), and the decay from the triplet state (k_t). (b) Numerical simulation of electric field intensity for a monomer (left) and dimer with an interparticle spacing of 23 nm (right) for 80-nm-diameter AuNPs. The excitation light at 640 nm is horizontally polarized.[1] (c) Schematic representation of 20 nm AuNP on 2D rectangular DNA origami. (d–f) Changes in the decay rates (indicated with an apostrophe) for the sample with dye–NP separations of 27.8 nm (cyan circles) and of 8.3 nm (black circles) are normalized to the mean value of the population without NP.[21] For the 8.3 nm sample, two populations are visible as not all DNA origami carry an NP. τ_{Fl} is the fluorescence lifetime. (g) Schematic representation of 20–100 nm AuNP on 3D pillar DNA origami. (h–j) All relevant photophysical rates are enhanced with increasing particle size (blue, experimental data; black, theoretical simulations).[21]

diagnostics and single-molecule (SM) fluorescence experiments.

FUNDAMENTAL ASPECTS OF INTERACTIONS BETWEEN FLUOROPHORES AND NANOPARTICLES

In the last years, DNA origami has emerged as a modular platform to study the fluorophore–NP interactions at the SM level. To this end, DNA nanostructures containing biotin modifications can be immobilized on glass surfaces, and NPs, functionalized with ssDNA via thiol-Au/Ag interactions,[17] can be annealed to complementary strands protruding from the DNA origami at the designed positions (Figure 1b).

The dye–plasmonic NP interaction depends on the NP size, shape, and material and also on the distance (d) and orientation between the dye and the NP.[10] Whether the emission of a fluorophore is enhanced or quenched in the vicinity of a plasmonic NP is determined by the extent to which the altered local electric field affects its photophysical properties (i.e., the excitation (k_{ex}), radiative (k_r), and nonradiative (k_{nr}) decay rates (Figure 2a)). All of these processes together with the electric field enhancement in the vicinity of plasmonic NPs can be approximated by numerical simulations (Figure 2b).[18]

In 2012, Acuna et al. addressed the distance-dependent interaction between a 10 nm AuNP and a single ATTO647N dye using a rectangular 2D DNA nanostructure (Figure 2c).[19] It was demonstrated that the quenching of fluorophores by AuNPs is strongly dependent on their spatial separation. This dependence deviated from the $1/d^4$ distance dependence that is characteristic of nanosurface energy transfer (NSET)[20] and exceeded the typical fluorescence resonance energy transfer (FRET) distances (4–8 nm), showing 50% intensity quenching at 10.4 nm. This phenomenon was further investigated by Holzmeister et al.,[21] who demonstrated that while k_{ex} and k_r of a dye in the vicinity of a 20 nm AuNP are not strongly affected, k_{nr} is very sensitive to the distance to the NP (Figure 2c–f). In contrast, when an ATTO647N dye is placed in the equatorial plane of larger AuNPs with respect to the direction of the excitation using a pillar-shaped 3D DNA origami, an enhancement of the excitation field and photophysical rates (k_{ex}, k_r, and k_{nr}) was observed (Figure 2b,g–j).[21,22] This is reflected in a shorter fluorescence lifetime (Figures 2d–f and 3a,c).[1,4,21,22] The increase in k_{nr} is usually

https://doi.org/10.1021/acs.accounts.1c00307
Acc. Chem. Res. 2021, 54, 3338–3348

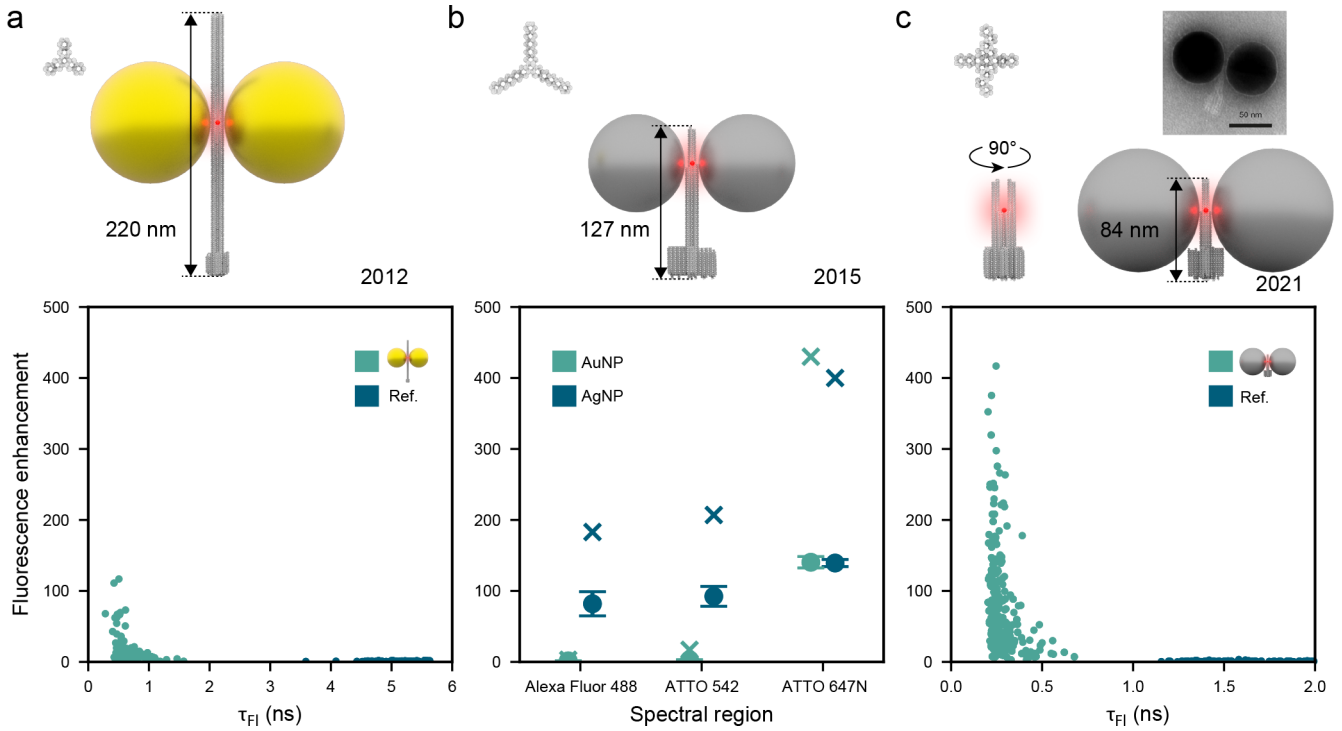

Figure 3. Evolution of DNA origami nanoantennas for fluorescence enhancement. (a) Pillar-shaped DNA origami structure and FE obtained for ATTO647N in the hotspot of dimer 100 nm AuNPs NA (green) in comparison to a reference structure (blue) containing no NPs.[1] (b) Pillar-shaped DNA origami and FE of dyes from different parts of the visible spectrum in the hotspot of dimer 100 nm AuNPs (green) and 80 nm AgNPs (blue) NAs.[2] Measurements were performed on a wide-field microscope which does not provide fluorescence lifetime (τ_{Fl}) information. The monomer subpopulation was excluded from the distribution based on FE values. Dots represent the mean experimental FE with the standard error, and crosses represent the maximal obtained FE values. (c) NACHOS provide a free space in the plasmonic hotspot for placing biomolecular assays.[4] TEM image of NACHOS with 60 nm AuNP (top). FE obtained on a confocal microscope for Alexa Fluor 647 in the hotspot of dimer 100 nm AgNPs NA (green) in comparison to a reference structure (blue) containing no NPs.

attributed to the energy transfer to dark modes of NPs.[10] Earlier studies have demonstrated that the intrinsic intersystem crossing rate (k_{ISC}) does not change in the presence of plasmonic particles,[23] while the influence on other nonradiative decay pathways (e.g., internal conversion k_{IC}), to the best of our knowledge, has not been reported. The 3D pillar-shaped DNA origami also allowed us to study the angular fluorescence intensity modulation of a single Cy5 dye close to a 40 or 80 nm AuNP, revealing the polarization-dependent enhancement and quenching of fluorescence emission.[22] Toward beam-steering nanoantennas, we also demonstrated that the emission of a freely rotating Cy5 dye in the gap of dimer Au NA can be directed by plasmonic effects and follows a dipolar pattern.[24]

These findings were key in improving our understanding of the interplay between fluorophores and plasmonic NPs. We found that there is an optimal distance and orientation between the dye and the NP surface and that controlling these parameters is pivotal for achieving high FE in DNA NAs. Here we provide a list of the factors that are helpful to consider when designing optical DNA NAs for FE:

1. Particle Size. As a first approximation, fluorescence quenching scales with particle volume, while fluorescence enhancement scales with the square of the volume.[25] This means that the particles should be chosen to be as large as possible under consideration of other effects, such as retardation, which impose an upper limit on the particle size.[26] In our hand, the highest enhancement factors were achieved with 100 nm particles.

2. Gap Size. The smaller the gap between NPs, the higher the electric field enhancement.[27] However, this also results in more red-shifted plasmon resonance. The dye should not be placed too close to the NP because in this regime the nonradiative decay pathways would outcompete the radiative decay and quenching rather than fluorescence enhancement would be observed.[19,27]

3. Excitation and Emission Spectra. The excitation and emission enhancements are governed by the spectral overlap with the plasmonic near-field, which is typically red-shifted from the far-field (scattering) spectrum.[25]

4. Orientation. The dye has to be in the equatorial plane (as shown in Figure 2g) of the incident light in order to be exposed to the maximum possible electrical field, and the dipole of the molecule should be oriented parallel to the dipole of the NA.[21,28] Also, excitation polarization has to be aligned with the plasmon longitudinal mode in plasmonic structures with nonspherical symmetry.

FORMING AND CONTROLLING PLASMONIC HOTSPOTS FOR FLUORESCENCE ENHANCEMENT

On the basis of previously formulated principles,[12,21,28,29] the first FE studies with DNA origamis were performed on a 3D pillar-shaped DNA nanostructure (Figure 2g). Here, FEs of 5- and 8-fold were obtained for a single Cy5 dye at a distance of ~12 nm to single 40 and 80 nm AuNPs, respectively.[22] However, it was evident from other studies that much higher FE values could be achieved if the dye could be placed in the gap between two or more plasmonic NPs (Figure 2b).[30]

https://doi.org/10.1021/acs.accounts.1c00307
Acc. Chem. Res. 2021, 54, 3338−3348

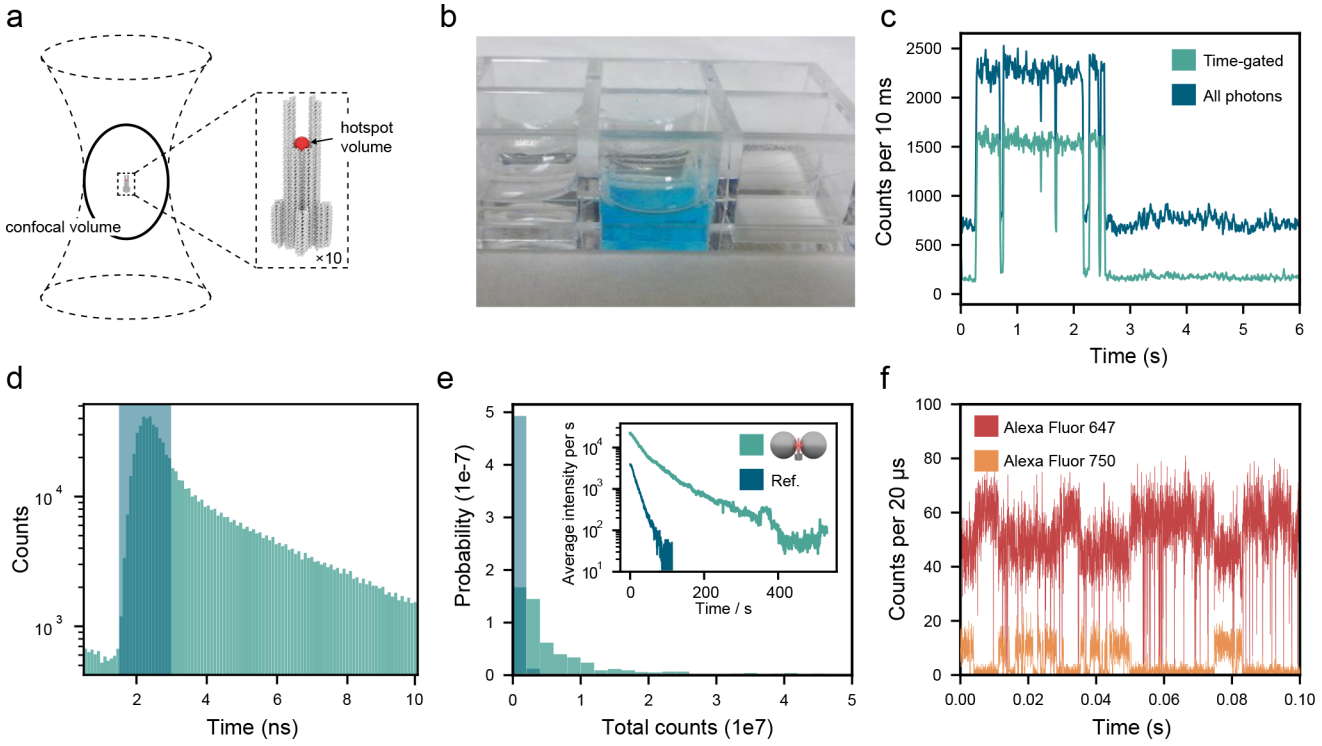

Figure 4. (a) Typical confocal detection volume compared to the plasmonic hotspot (indicated in red) of an NA. (b) Photograph of a sample chamber containing 25 μM ATTO647N.[27] (c, d) Fluorescence transient of ATTO647N in the plasmonic hotspot at 0.5 μM ATTO647N background.[1] Lifetime gating improves the contrast as molecules in the hotspot have a shorter fluorescence decay (dark blue) while omitting the majority of background photons. (e) Photon budget and average fluorescence intensity over time (inset) of ATTO647N in the reference DNA origami structure (excited at 639 nm, 9 mW) as well as in the hotspot of dimer 100 nm AuNP NA (excited at 639 nm, 1.6 mW).[37] (f) High-resolution FRET transient showing fluctuations induced by acceptor blinking enabled by plasmonic-enhanced fluorescence. Photon count rates of 3.5 MHz (donor, red) and 1 MHz (acceptor, orange) are achieved.

The first study utilizing the DNA origami technique to create such self-assembled dimer plasmonic NAs and to place a single dye in the plasmonic hotspot was reported in 2012 by Acuna et al. In this study, the authors designed a pillar-shaped DNA origami[1] and prepared dimer NAs with AuNPs of different sizes (20−100 nm). In line with theoretical predictions, 100 nm dimer NAs with an interparticle gap of ∼23 nm demonstrated the highest FE factors, reaching 117-fold (Figure 3a).

To improve the FE, the design of the DNA origami evolved over the next few years (Figure 2b,c), aiming to maintain the vertical orientation of the structure for better alignment of the NP's dipole with the polarization of the incident light[31] and decreasing the interparticle distance by narrowing down the top of the structure to a six-helix bundle (Figure 3b). Further improvements in NA preparation included overcoming the aggregation of larger NPs[32] by using longer ssDNA for functionalization and exploiting the zipper-binding geometry (Figure 1d) to decrease the distance between NPs to 12−17 nm and hence obtain a higher electric field enhancement[26,27] (Figure 1c). These improvements made it possible to obtain FE values of up to 471-fold for a dimer 100 nm AuNP NA.[27] A further increase in NP size did not lead to further improvement in FE due to retardation effects and red-shifted plasmon resonance.[26]

The next step forward in expanding the utility of the plasmonic hotspot was the demonstration of broadband FE with self-assembled AgNP optical antennas.[2] NAs based on AuNPs provide FE typically in the red and near-infrared spectral regions. In contrast, AgNPs have a plasmon resonance in the violet-blue spectral region (which can be red-shifted upon their dimerization),[33] allowing their coupling with dyes that span a broad spectral range. Using the improved protocol for large NP functionalization,[26] Vietz et al. used AgNPs to assemble optical NAs, demonstrating FE of up to 2 orders of magnitude for dyes spanning almost the whole visible spectrum (Figure 3b).[2]

On the one hand, the rigid DNA structure between the NPs ensures a well-defined hotspot. The drawback of this NA design, however, is the fact that the majority of the plasmonic hotspot region was blocked by the DNA origami structure itself, which prevents the incorporation of larger biomolecules or biological assays.[3,34] This problem was recently addressed by a newly designed 3D DNA origami, named NACHOS (Figure 3c), which provides a free space in the plasmonic hotspot region formed by two 100 nm AuNPs or AgNPs. As discussed later, this enabled placing biomolecular assays in the plasmonic hotspot while maintaining high FE reaching >400-fold.[4]

One of the main challenges we faced over the years was the heterogeneity of FE distributions, which reflect the heterogeneity in NP size and shape,[35] and the different orientations of NAs with respect to the excitation field. The FE distributions shown also contain a subpopulation of monomer NAs, characterized by a lower FE and higher fluorescence lifetimes (Figure 3a,c; in Figure 3b the monomer contribution to FE values was filtered). Furthermore, one cannot reject the possibility of multimeric binding of NPs to the DNA origami,

https://doi.org/10.1021/acs.accounts.1c00307
Acc. Chem. Res. 2021, 54, 3338−3348

which in the future we hope to investigate further by correlative fluorescence/dark field/electron microscopy studies. While this heterogeneity does not pose a limitation for improving SM detection (as long as even low FE values are bright enough to detect them), it represents a challenge to extracting quantitative information when adapting the NAs to boost the fluorescence signals of common ensemble diagnostic assays. Possible strategies to address this heterogeneity problem might include exploiting more homogeneous NPs,[36] developing strategies to achieve better coalignment of NA and dye dipoles as well as even more defined and rigid positioning of NPs.

DNA ORIGAMI NANOANTENNAS FOR SINGLE-MOLECULE BIOPHYSICS

The ability to position molecules precisely in the plasmonic hotspot paved the way toward exciting new applications in the field of SM biophysics. DNA NAs provide three clear advantages for SM imaging: (1) an enhanced fluorescence signal of a single emitter allows imaging at higher background concentrations of fluorophores; (2) higher count rates by FE enable higher time resolution; and (3) fast depopulation of the excited states in the hotspot improves the photostability of fluorescent labels.

The first advantage is central to a long-lasting problem in the field: the discrepancy between the concentrations needed for SM detection (which are in the pM to nM range) and the concentration range in which most biomolecules are present and active *in vivo* (usually in the μM to mM range).[38] Strategies to overcome this problem include the use of elaborate microfluidic setups or highly confined observation volumes (e.g., zero mode wave guides,[39] the "antenna in a box" platform,[40] convex lens-induced confinement (CLIC),[41] or nanopipettes[42]).

With DNA NAs, an alternative and more straightforward way has emerged. The significantly reduced excitation volume is the key: a plasmonic hotspot typically is on the order of zL, while typical confocal excitation volumes are on the order of fL, a million times larger. Thus, by reducing the effective excitation volume, the background fluorescence can be decreased significantly (Figure 4a). Additionally, the reduced fluorescence lifetime of emitters in the plasmonic hotspot enables a further cleanup step by time-gating the photons (Figure 4c,d).[1] With this, SM detection has been shown to be feasible even in solutions containing micromolar concentrations of fluorophores (Figure 4b−d), extending SM fluorescence experiments to biologically relevant concentration ranges.

Enhancing the photostability of fluorophores is of great importance for all SM fluorescence experiments because the amount of information that can be extracted is fundamentally limited by the survival time of the dye molecule. The increase in photostability strongly correlates with the increase in the radiative rate k_r[29] (an up to 75-fold increase in k_r has been shown in a plasmonic hotspot),[43] which results in a vastly reduced time that the fluorophore spends in reactive excited states[37] and therefore a decrease of the probability of processes leading to photobleaching. The lifetimes of triplet excited states of fluorophores (common intermediates in the photobleaching pathways as well as precursors of singlet oxygen and other reactive oxygen species) have also been shown to be reduced in the vicinity of plasmonic nanostructures,[44−46] which could further contribute to improved photostability in plasmonic hotspots. Pellegrotti et al.,[29] for example, demonstrated that a Cy5 dye positioned close the surface of a 80 nm AuNP on average emits more than 4 times more photons before photobleaching. Another study utilizing 80 nm AgNP dimer NAs showed that the photostability of a blue-absorbing fluorophore (Alexa Fluor 488) can also be increased by >30-fold.[47] More recently, we have also demonstrated an up to 40-fold increase in the total photon budget in DNA NA containing two 100 nm Ag NP for one of the most photostable organic dyes—ATTO647N—which could potentially be further increased by additional photostabilizers in solution (Figure 4e). We have also found that the saturation behavior of dyes is affected when placed in the hotspots of plasmonic NAs, with the maximum photon count rates that can be achieved being limited and specific to the nature of the fluorophore that is used.[37]

Plasmonic effects can also improve the time resolution of FRET experiments. Many interesting biological processes such as protein folding and aggregation occur on the submillisecond time scale, which is hard to access via conventional methods. Proteins are therefore approximated by two-state systems, but the wealth of information on what happens during the transition from the folded to the unfolded state or vice versa is often hidden. Here, the limiting factor is not the photon budget but the maximum number of detected photons per unit time (the photon count rate). Even with the most elaborate chemical photostabilization procedures, photon count rates achievable with the best fluorophores are usually below 1000 ms^{-1} and the dyes survive only for several milliseconds before photobleaching.[48,49] As illustrated in Figure 4f, plasmonic effects can also increase the count rates substantially in single-molecule FRET experiments, enabling real-time visualization of transitions on the millisecond to microsecond time scale. The presented transient showing FRET fluctuations induced by acceptor blinking could be followed for 5 s before photobleaching.

In combination with newly developed organic dyes that are spectrally more stable and show reduced blinking behavior on short time scales,[50,51] this opens up exciting new research directions as fast nonequilibrium dynamics such as barrier crossing events in protein folding[52] could become accessible with this increased time resolution.

DNA ORIGAMI NANOANTENNAS FOR DIAGNOSTICS

Many fluorescence-based molecular diagnostic assays, in particular, those used to detect low-abundance analytes, require molecular amplification of target molecules (e.g., polymerase chain reaction or sandwich ELISA assays).[53] Physical amplification of the signal upon detection of single target molecules could provide the means to improve the speed, robustness, and multiplexing capabilities of these assays and overcome the problem of a low signal-to-background ratio originating from the background signal of the large number of other molecules present in the observation volume (e.g., due to scattering, autofluorescence, and nonspecific binding).[53] It could also open possibilities to detect single molecules on much cheaper and simpler devices, enabling ultrasensitive detection in point-of-care diagnostic settings.[54] When aiming at enhancing the signal of a molecular assay with the help of plasmonic NAs, one is faced with an obvious challenge: how to place this assay directly in the plasmonic hotspot. In contrast to other surface-enhanced spectroscopies, the gap between the

https://doi.org/10.1021/acs.accounts.1c00307
Acc. Chem. Res. 2021, 54, 3338−3348

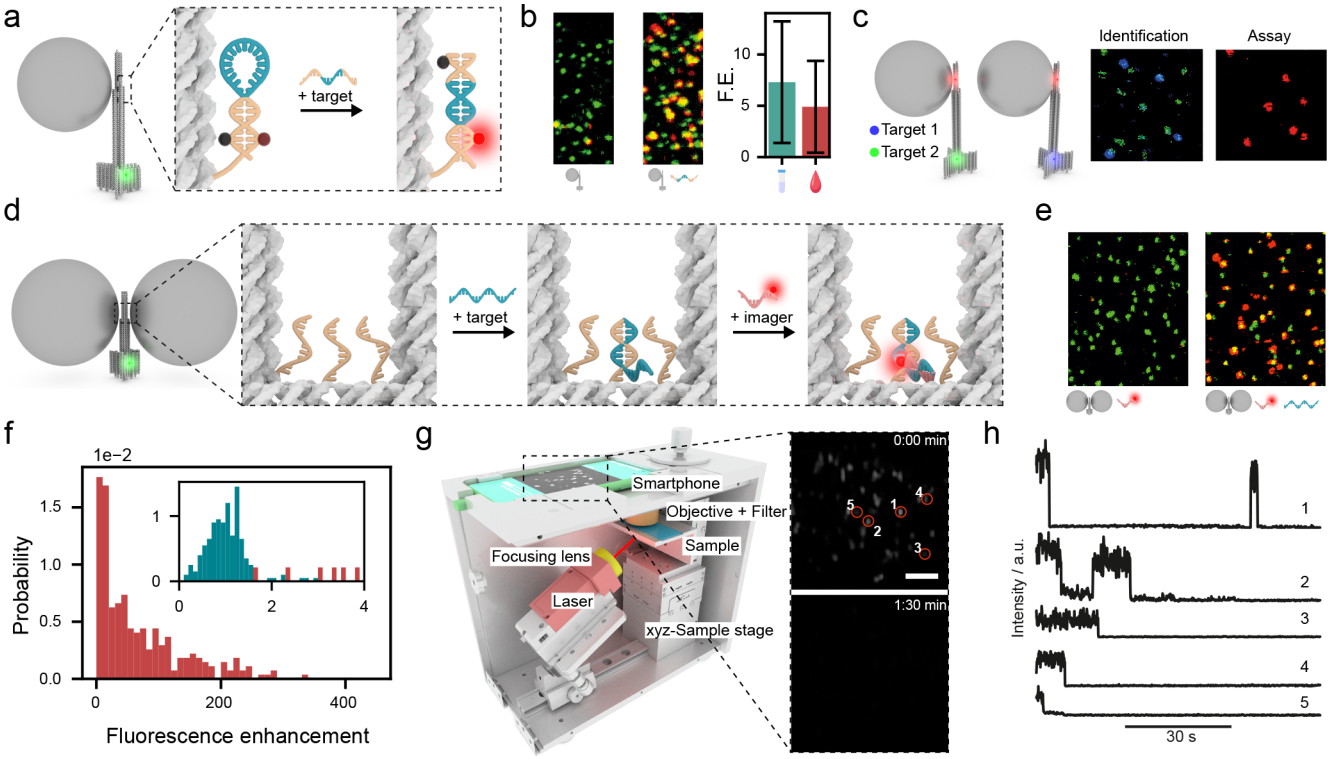

Figure 5. (a) Sketch of the FQH assay designed to detect DNA and RNA specific to the Zika virus.[3] (b) Confocal fluorescence scans in heat-deactivated blood serum in the absence and presence of DNA specific to the Zika virus obtained for NA structures (DNA origami containing 80 nm AgNP) and corresponding FE that could be achieved in buffer as well as in blood serum.[3] (c) Strategy to achieve multiplexing with NAs by barcoding the DNA origami structures with different dyes (left) and confocal fluorescence scans of the multiplexed detection of two different DNA targets (right).[3] (d) Sketch of the sandwich binding assay in the hotspot of NACHOS designed to detect DNA specific to antibiotic-resistant bacteria.[4] (e) Fluorescence scans of the sandwich binding assay in heat-deactivated blood serum in the absence and presence of the DNA target (left and right panels, respectively).[4] (f) FE obtained in the sandwich binding assay with NACHOS in heat-deactivated blood serum.[4] The inset shows the intensity distribution of single fluorophores, illustrating the power of NACHOS to distinguish the target-specific signal from SM impurities. (g) Home-built portable smartphone microscope used to detect single DNA molecules on a smartphone camera with the help of NACHOS (left) and snapshots of the movie obtained on the smartphone camera (right).[4] (h) Fluorescence intensity vs time transients obtained in the sandwich detection assay (one to three dyes in the hotspot) extracted from the movie shown in g.[4]

nanoparticles in our DNA NAs is usually larger than 10 nm, with the potential to place biomolecular assays in the hotspot. DNA staple strands protruding from the DNA origami directly in the plasmonic hotspot can anchor biomolecular assays.

The first example of a diagnostic DNA NA comprised a pillar-shaped DNA origami (Figure 3b) containing a fluorescence-quenching hairpin (FQH) positioned near the 80 nm AgNP (Figure 5a). In the absence of the target molecule, the hairpin is in its closed state where the fluorescence of reporter dye ATTO647N is quenched by a BlackBerry quencher 650 (BBQ650). Upon binding of the target molecule (DNA or RNA specific to the Zika virus), the hairpin opened, separating the fluorophore and the quencher and generating a fluorescence signal which is amplified by the AgNP (Figure 5b, left). Using this AgNP NA, a specific DNA target could be detected not only in the buffer but also in heat-deactivated human serum with average FE values of 7.3 and 4.9, respectively (Figure 5b, right). Furthermore, by exploiting the modularity of DNA origami and additionally incorporating different fluorophores as barcodes in the base of the NA, two different DNA sequences could be detected simultaneously in one experiment (Figure 5c), demonstrating the multiplexing potential of this DNA NA approach.

One of the main limitations of this NA design (Figure 5a) for diagnostic applications was its moderate FE. Because of the limited accessibility of the hotspot region (Figure 3a,b) and steric constraints imposed by the DNA origami, only monomer NAs could be obtained, limiting FE values to several fold (Figure 5c).

This motivated us to design NACHOS (Figure 3c), which are the next-generation NAs specifically designed for the incorporation of larger biomolecular assays.[4] In contrast to previous NA designs, where the hotspot region is almost completely blocked by the DNA nanostructure (Figure 3a,b), the design used for NACHOS has the hotspot region cleared from DNA (Figure 3c). Even upon the binding of 100 nm NPs, different target molecules can access the plasmonic hotspot from above (Figure 3c). To avoid false positive events that we experienced in the hairpin assay due to dark-quencher bleaching,[37] we switched to a sandwich binding assay (Figure 5d) that was incorporated into the hotspot to detect a DNA fragment specific to *OXA-48* (used for the diagnosis of an infection with antibiotic-resistant Klebsiella pneumonia).[55,56] Three 17-nucleotide-long capture strands complementary to a part of the target DNA were designed to protrude directly into the plasmonic hotspot of the NACHOS (Figure 5d). Binding of the target DNA sequence then provides an overhang for the 17-nt-long fluorophore-labeled imager strand to be incorporated directly into the plasmonic hotspot where the signal of the reporter dye is amplified by the NA.

https://doi.org/10.1021/acs.accounts.1c00307
Acc. Chem. Res. 2021, 54, 3338−3348

In the base of NACHOS, we incorporated green dye ATTO542 to visualize colocalization with imager strands (red) that target detection (Figure 5d). DNA specific to *OXA-48* was detected in buffer as well as in heat-deactivated blood serum (Figure 5e, right) with a very low extent (~2.5%) of false positive signal observed in the absence of the target (Figure 5e, left). Because of the successful formation of dimer NAs, FE reaching up to 461-fold (average of 89 ± 7-fold) could be achieved for this diagnostic assay (Figure 5f), representing more than an order of magnitude improvement compared to the previous design discussed above. One advantage of using NACHOS in combination with the sandwich binding assay is that it allows for a clear differentiation between the amplified signal originating from specific target binding in the zL volume of the NA hotspot and the nonamplified signal from single fluorescent emitters (Figure 5f, inset on the right). This allows us to address one of the major challenges of SM diagnostics, that is, to distinguish positive signals from unavoidable impurities and nonspecific binding.

The high signal amplification provided by NACHOS also enabled us to demonstrate for the first time that single DNA targets can be detected on a portable smartphone microscope.[4] The custom-built smartphone microscope contained a laser, cheap and nonspecialized low-NA optics, and a Huawei P20 smartphone for detection (Figure 5g). After showing that the FE is sufficient to enable the detection of single fluorophores on the smartphone camera, we also carried out the sandwich detection assay (Figure 5g) using this portable and power-bank-driven device. Fluorescence intensity vs time transients extracted from the smartphone movies demonstrated that the bleaching of one to three dyes incorporated in the hotspot NACHOS was detected on the smartphone camera (Figure 5h), highlighting the ability of the smartphone microscope in combination with NACHOS to provide analytical power comparable to conventional SM microscopy tools.

CONCLUSIONS AND OUTLOOK

Recent years saw the coming of age of DNA nanotechnology, and its impact on several disciplines has undoubtedly been outstanding. Specifically, the field of plasmonics has profited tremendously from the positioning capabilities of the DNA origami technique, with astonishing discoveries made by many groups around the world.[57−61] In our line of work, we focused on harnessing the power of the approach for FE purposes. We have discovered several intricacies of the interplay between the plasmonic NPs and fluorophores which would have been difficult to address with any other approach. These mechanistic insights enabled us to build plasmonic NAs that can enhance the signals of single emitters by up to several hundred times and for the first time demonstrate that a single fluorophore could be "seen" simply with a smartphone camera. An exciting future direction could involve the use of these DNA NAs for SM detection on even cheaper and more miniaturized devices and their incorporation with high-throughput microfluidic and surface-spotting approaches. Moreover, one could also explore the advantages of other geometries of plasmonic nanostructures (e.g., Au or Ag nanorods which could lead to potentially even higher FEs).

Over the years, our efforts in using DNA NAs for diagnostic purposes have developed from a very basic proof-of-concept level[3] toward a viable alternative or augmentation of other diagnostic assays.[4] Early versions of our DNA NAs suffered from low dimer yields and very heterogeneous enhancement profiles,[1] and although tremendous progress has been made in this regard, further improvements in this direction are necessary to use our NA assay not only in a qualitative "yes or no"-type manner but also to gain quantitative information about the analyte, as is needed in many diagnostic settings.[53] When it comes to the ultrasensitive detection of biomarkers, another consideration is that signal amplification might simply not be sufficient to detect targets at concentrations in the aM−fM range, and efficient approaches to capturing the few target copies present in milliliters of blood are also necessary.[53,62] To diversify the range of targets that can be detected with DNA NAs, assays will be required to go beyond the detection of DNA and RNA.[53] We are currently exploring different approaches to how this could be implemented (e.g., by incorporating nanoswitches[63] in the hotspots of NAs for the specific detection of antibodies).

With our understanding of the control of DNA NAs, other ideas moved closer to the scope of reality. It has been anticipated that DNA NAs might have great use in biophysical experiments because of their ability to decrease the effective observation volume,[64] to increase the time resolution, and to increase the photostability of the fluorescent reporters.[29,37,47,65] We have already shown that we can observe the switching of a DNA Holliday junction via FRET at extremely low excitation powers.[1] We also studied the effect of the plasmonic effect on the FRET process[66] and concluded that it should be possible to enhance the overall photon count rate of a FRET assay using DNA NAs. Ongoing work is focusing on exploring these directions with the aim of entering the lower microsecond time scales previously inaccessible to SM fluorescence imaging and providing new mechanistic insights on fast processes such as protein folding and the conformational dynamics of biomolecules.

AUTHOR INFORMATION

Corresponding Author

Philip Tinnefeld − *Department of Chemistry and Center for NanoScience, Ludwig-Maximilians-Universität München, 81377 München, Germany;* orcid.org/0000-0003-4290-7770; Email: philip.tinnefeld@cup.lmu.de

Authors

Viktorija Glembockyte − *Department of Chemistry and Center for NanoScience, Ludwig-Maximilians-Universität München, 81377 München, Germany;* orcid.org/0000-0003-2531-6506

Lennart Grabenhorst − *Department of Chemistry and Center for NanoScience, Ludwig-Maximilians-Universität München, 81377 München, Germany;* orcid.org/0000-0001-9503-1819

Kateryna Trofymchuk − *Department of Chemistry and Center for NanoScience, Ludwig-Maximilians-Universität München, 81377 München, Germany;* orcid.org/0000-0003-3453-1320

Complete contact information is available at: https://pubs.acs.org/10.1021/acs.accounts.1c00307

Author Contributions

†V.G., L.G., and K.T. contributed equally to this work.

Notes

The authors declare no competing financial interest.

https://doi.org/10.1021/acs.accounts.1c00307
Acc. Chem. Res. 2021, 54, 3338−3348

Biographies

Viktorija Glembockyte is currently a Marie Skłodowska-Curie Research Fellow at Ludwig-Maximilians-Universität (LMU) München (Germany). She studied chemistry at Jacobs University Bremen (Germany) and obtained a Ph.D. in chemistry from McGill University (Canada) in 2017. In her current research, she combines the advantages of DNA nanotechnology and SM fluorescence imaging for the development of diagnostic tools and tunable biosensors.

Lennart Grabenhorst studied biochemistry in Göttingen (B.Sc.) and Braunschweig (M.Sc.) and is currently a Ph.D. student in Philip Tinnefeld's group at LMU Munich. His research interests include SM fluorescence spectroscopy, biophysics, DNA nanotechnology, and plasmonics.

Kateryna Trofymchuk is currently a postdoctoral researcher at LMU Munich (Germany). She studied physics at Taras Shevchenko National University of Kyiv (Ukraine) and obtained a Ph.D. in physics from University of Strasbourg (France) in 2016. Her current research is focused on combining the advantages of DNA nanotechnology and SM fluorescence imaging for the development of diagnostic tools.

Philip Tinnefeld has been a professor of physical chemistry at LMU since 2017. He studied chemistry at Münster and Heidelberg and received his Ph.D. from the University of Heidelberg in 2002. After postdoctoral work at UCLA (United States) and Leuven (Belgium) and habilitation in physics at Bielefeld University, he became associate professor of biophysics at LMU Munich. In 2010, he was appointed full professor of biophysical chemistry at TU Braunschweig. His research is inspired by our emerging abilities to study and build matter from the bottom up, starting from single molecules. He has contributed to breakthroughs of single-molecule superresolution microscopy, and he combined optical SM detection with DNA nanotechnology for self-assembled, functional devices including energy-transfer switches, calibration nanorulers, nanoadapters, fluorescence signal amplifiers, and molecular force clamps.

■ ACKNOWLEDGMENTS

P.T. gratefully acknowledges financial support from the DFG (TI 329/9-1, TI 329/9-2, INST 86/1904-1 FUGG, excellence clusters NIM, and e-conversion), Sino-German Center for Research Promotion (grant agreement C-0008), BMBF (grants POCEMON, 13N14336, and SIBOF, 03VP03891). V.G. acknowledges support from the European Union's Horizon 2020 research and innovation program under the Marie Skłodowska-Curie actions (grant agreement no. 840741). V.G. and K.T. acknowledge the support by Humboldt Research Fellowships from the Alexander von Humboldt Foundation.

■ REFERENCES

(1) Acuna, G. P.; Möller, F. M.; Holzmeister, P.; Beater, S.; Lalkens, B.; Tinnefeld, P. Fluorescence Enhancement at Docking Sites of DNA-Directed Self-Assembled Nanoantennas. *Science* **2012**, *338*, 506−510.
(2) Vietz, C.; Kaminska, I.; Sanz Paz, M.; Tinnefeld, P.; Acuna, G. P. Broadband Fluorescence Enhancement with Self-Assembled Silver Nanoparticle Optical Antennas. *ACS Nano* **2017**, *11*, 4969−4975.
(3) Ochmann, S. E.; Vietz, C.; Trofymchuk, K.; Acuna, G. P.; Lalkens, B.; Tinnefeld, P. Optical Nanoantenna for Single Molecule-Based Detection of Zika Virus Nucleic Acids without Molecular Multiplication. *Anal. Chem.* **2017**, *89*, 13000−13007.
(4) Trofymchuk, K.; Glembockyte, V.; Grabenhorst, L.; Steiner, F.; Vietz, C.; Close, C.; Pfeiffer, M.; Richter, L.; Schütte, M. L.; Selbach, F.; Yaadav, R.; Zähringer, J.; Wei, Q.; Ozcan, A.; Lalkens, B.; Acuna, G. P.; Tinnefeld, P. Addressable nanoantennas with cleared hotspots for single-molecule detection on a portable smartphone microscope. *Nat. Commun.* **2021**, *12*, 950.
(5) Purcell, E. M. Spontaneous Emission Probabilities at Radio Frequencies. *Phys. Rev.* **1946**, *69*, 681.
(6) Drexhage, K. H. Influence of a dielectric interface on fluorescence decay time. *J. Lumin.* **1970**, *1*−*2*, 693−701.
(7) Bharadwaj, P.; Deutsch, B.; Novotny, L. Optical Antennas. *Adv. Opt. Photonics* **2009**, *1*, 438−483.
(8) Novotny, L.; van Hulst, N. Antennas for light. *Nat. Photonics* **2011**, *5*, 83−90.
(9) Kinkhabwala, A.; Yu, Z.; Fan, S.; Avlasevich, Y.; Müllen, K.; Moerner, W. E. Large single-molecule fluorescence enhancements produced by a bowtie nanoantenna. *Nat. Photonics* **2009**, *3*, 654−657.
(10) Anger, P.; Bharadwaj, P.; Novotny, L. Enhancement and Quenching of Single-Molecule Fluorescence. *Phys. Rev. Lett.* **2006**, *96*, 113002.
(11) Kühn, S.; Håkanson, U.; Rogobete, L.; Sandoghdar, V. Enhancement of Single-Molecule Fluorescence Using a Gold Nanoparticle as an Optical Nanoantenna. *Phys. Rev. Lett.* **2006**, *97*, 017402.
(12) Chhabra, R.; Sharma, J.; Wang, H.; Zou, S.; Lin, S.; Yan, H.; Lindsay, S.; Liu, Y. Distance-dependent interactions between gold nanoparticles and fluorescent molecules with DNA as tunable spacers. *Nanotechnology* **2009**, *20*, 485201.
(13) Busson, M. P.; Rolly, B.; Stout, B.; Bonod, N.; Bidault, S. Accelerated single photon emission from dye molecule-driven nanoantennas assembled on DNA. *Nat. Commun.* **2012**, *3*, 962.
(14) Rothemund, P. W. Folding DNA to create nanoscale shapes and patterns. *Nature* **2006**, *440*, 297−302.
(15) Douglas, S. M.; Dietz, H.; Liedl, T.; Högberg, B.; Graf, F.; Shih, W. M. Self-assembly of DNA into nanoscale three-dimensional shapes. *Nature* **2009**, *459*, 414−418.
(16) Fromm, D. P.; Sundaramurthy, A.; Schuck, P. J.; Kino, G.; Moerner, W. E. Gap-Dependent Optical Coupling of Single "Bowtie" Nanoantennas Resonant in the Visible. *Nano Lett.* **2004**, *4*, 957−961.
(17) Mirkin, C. A.; Letsinger, R. L.; Mucic, R. C.; Storhoff, J. J. A DNA-based method for rationally assembling nanoparticles into macroscopic materials. *Nature* **1996**, *382*, 607−609.
(18) Taminiau, T. H.; Stefani, F. D.; van Hulst, N. F. Single emitters coupled to plasmonic nano-antennas: angular emission and collection efficiency. *New J. Phys.* **2008**, *10*, 105005.
(19) Acuna, G. P.; Bucher, M.; Stein, I. H.; Steinhauer, C.; Kuzyk, A.; Holzmeister, P.; Schreiber, R.; Moroz, A.; Stefani, F. D.; Liedl, T.; Simmel, F. C.; Tinnefeld, P. Distance Dependence of Single-Fluorophore Quenching by Gold Nanoparticles Studied on DNA Origami. *ACS Nano* **2012**, *6*, 3189−3195.
(20) Persson, B. N. J.; Lang, N. D. Electron-hole-pair quenching of excited states near a metal. *Phys. Rev. B: Condens. Matter Mater. Phys.* **1982**, *26*, 5409−5415.
(21) Holzmeister, P.; Pibiri, E.; Schmied, J. J.; Sen, T.; Acuna, G. P.; Tinnefeld, P. Quantum yield and excitation rate of single molecules close to metallic nanostructures. *Nat. Commun.* **2014**, *5*, 5356.
(22) Möller, F. M.; Holzmeister, P.; Sen, T.; Acuna, G. P.; Tinnefeld, P. Angular modulation of single-molecule fluorescence by gold nanoparticles on DNA origami templates. *Nanophotonics* **2013**, *2*, 167−172.
(23) Stefani, F. D.; Vasilev, K.; Bocchio, N.; Gaul, F.; Pomozzi, A.; Kreiter, M. Photonic mode density effects on single-molecule fluorescence blinking. *New J. Phys.* **2007**, *9*, 21−21.
(24) Hübner, K.; Pilo-Pais, M.; Selbach, F.; Liedl, T.; Tinnefeld, P.; Stefani, F. D.; Acuna, G. P. Directing Single-Molecule Emission with DNA Origami-Assembled Optical Antennas. *Nano Lett.* **2019**, *19*, 6629−6634.
(25) Taylor, A. B.; Zijlstra, P. Single-Molecule Plasmon Sensing: Current Status and Future Prospects. *ACS Sens* **2017**, *2*, 1103−1122.

https://doi.org/10.1021/acs.accounts.1c00307
Acc. Chem. Res. 2021, 54, 3338−3348

(26) Vietz, C.; Lalkens, B.; Acuna, G. P.; Tinnefeld, P. Functionalizing large nanoparticles for small gaps in dimer nanoantennas. *New J. Phys.* **2016**, *18*, 045012.
(27) Puchkova, A.; Vietz, C.; Pibiri, E.; Wünsch, B.; Sanz Paz, M.; Acuna, G. P.; Tinnefeld, P. DNA Origami Nanoantennas with over 5000-fold Fluorescence Enhancement and Single-Molecule Detection at 25 μM. *Nano Lett.* **2015**, *15*, 8354−8359.
(28) Lakowicz, J. R.; Fu, Y. Modification of single molecule fluorescence near metallic nanostructures. *Laser Photonics Rev.* **2009**, *3*, 221−232.
(29) Pellegrotti, J. V.; Acuna, G. P.; Puchkova, A.; Holzmeister, P.; Gietl, A.; Lalkens, B.; Stefani, F. D.; Tinnefeld, P. Controlled reduction of photobleaching in DNA origami-gold nanoparticle hybrids. *Nano Lett.* **2014**, *14*, 2831−2836.
(30) Li, K.; Stockman, M. I.; Bergman, D. J. Self-Similar Chain of Metal Nanospheres as an Efficient Nanolens. *Phys. Rev. Lett.* **2003**, *91*, 227402.
(31) Schmied, J. J.; Forthmann, C.; Pibiri, E.; Lalkens, B.; Nickels, P.; Liedl, T.; Tinnefeld, P. DNA Origami Nanopillars as Standards for Three-Dimensional Superresolution Microscopy. *Nano Lett.* **2013**, *13*, 781−785.
(32) Zhang, X.; Servos, M. R.; Liu, J. Instantaneous and Quantitative Functionalization of Gold Nanoparticles with Thiolated DNA Using a pH-Assisted and Surfactant-Free Route. *J. Am. Chem. Soc.* **2012**, *134*, 7266−7269.
(33) Coronado, E. A.; Encina, E. R.; Stefani, F. D. Optical properties of metallic nanoparticles: manipulating light, heat and forces at the nanoscale. *Nanoscale* **2011**, *3*, 4042−4059.
(34) Vietz, C.; Lalkens, B.; Acuna, G. P.; Tinnefeld, P. Synergistic Combination of Unquenching and Plasmonic Fluorescence Enhancement in Fluorogenic Nucleic Acid Hybridization Probes. *Nano Lett.* **2017**, *17*, 6496−6500.
(35) Tian, L.; Wang, C.; Zhao, H.; Sun, F.; Dong, H.; Feng, K.; Wang, P.; He, G.; Li, G. Rational Approach to Plasmonic Dimers with Controlled Gap Distance, Symmetry, and Capability of Precisely Hosting Guest Molecules in Hotspot Regions. *J. Am. Chem. Soc.* **2021**, *143*, 8631−8638.
(36) Yoon, J. H.; Selbach, F.; Langolf, L.; Schlücker, S. Ideal Dimers of Gold Nanospheres for Precision Plasmonics: Synthesis and Characterization at the Single-Particle Level for Identification of Higher Order Modes. *Small* **2018**, *14*, 1702754.
(37) Grabenhorst, L.; Trofymchuk, K.; Steiner, F.; Glembockyte, V.; Tinnefeld, P. Fluorophore photostability and saturation in the hotspot of DNA origami nanoantennas. *Methods Appl. Fluoresc.* **2020**, *8*, 024003.
(38) Holzmeister, P.; Acuna, G. P.; Grohmann, D.; Tinnefeld, P. Breaking the concentration limit of optical single-molecule detection. *Chem. Soc. Rev.* **2014**, *43*, 1014−1028.
(39) Levene, M. J.; Korlach, J.; Turner, S. W.; Foquet, M.; Craighead, H. G.; Webb, W. W. Zero-Mode Waveguides for Single-Molecule Analysis at High Concentrations. *Science* **2003**, *299*, 682−686.
(40) Punj, D.; Mivelle, M.; Moparthi, S. B.; van Zanten, T. S.; Rigneault, H.; van Hulst, N. F.; García-Parajó, M. F.; Wenger, J. A plasmonic 'antenna-in-box' platform for enhanced single-molecule analysis at micromolar concentrations. *Nat. Nanotechnol.* **2013**, *8*, 512−516.
(41) Leslie, S. R.; Fields, A. P.; Cohen, A. E. Convex Lens-Induced Confinement for Imaging Single Molecules. *Anal. Chem.* **2010**, *82*, 6224−6229.
(42) Vogelsang, J.; Doose, S.; Sauer, M.; Tinnefeld, P. Single-Molecule Fluorescence Resonance Energy Transfer in Nanopipets: Improving Distance Resolution and Concentration Range. *Anal. Chem.* **2007**, *79*, 7367−7375.
(43) Schedlbauer, J.; Wilhelm, P.; Grabenhorst, L.; Federl, M. E.; Lalkens, B.; Hinderer, F.; Scherf, U.; Höger, S.; Tinnefeld, P.; Bange, S.; Vogelsang, J.; Lupton, J. M. Ultrafast Single-Molecule Fluorescence Measured by Femtosecond Double-Pulse Excitation Photon Antibunching. *Nano Lett.* **2020**, *20*, 1074−1079.
(44) Wientjes, E.; Renger, J.; Cogdell, R.; van Hulst, N. F. Pushing the Photon Limit: Nanoantennas Increase Maximal Photon Stream and Total Photon Number. *J. Phys. Chem. Lett.* **2016**, *7*, 1604−1609.
(45) Pacioni, N. L.; González-Béjar, M.; Alarcón, E.; McGilvray, K. L.; Scaiano, J. C. Surface Plasmons Control the Dynamics of Excited Triplet States in the Presence of Gold Nanoparticles. *J. Am. Chem. Soc.* **2010**, *132*, 6298−6299.
(46) Kéna-Cohen, S.; Wiener, A.; Sivan, Y.; Stavrinou, P. N.; Bradley, D. D. C.; Horsfield, A.; Maier, S. A. Plasmonic Sinks for the Selective Removal of Long-Lived States. *ACS Nano* **2011**, *5*, 9958−9965.
(47) Kaminska, I.; Vietz, C.; Cuartero-González, Á.; Tinnefeld, P.; Fernández-Domínguez, A. I.; Acuna, G. P. Strong plasmonic enhancement of single molecule photostability in silver dimer optical antennas. *Nanophotonics* **2018**, *7*, 643−649.
(48) Campos, L. A.; Liu, J.; Wang, X.; Ramanathan, R.; English, D. S.; Munoz, V. A photoprotection strategy for microsecond-resolution single-molecule fluorescence spectroscopy. *Nat. Methods* **2011**, *8*, 143−146.
(49) van der Velde, J. H. M.; Smit, J. H.; Hebisch, E.; Punter, M.; Cordes, T. Self-healing dyes for super-resolution fluorescence microscopy. *J. Phys. D: Appl. Phys.* **2019**, *52*, 034001.
(50) Michie, M. S.; Gotz, R.; Franke, C.; Bowler, M.; Kumari, N.; Magidson, V.; Levitus, M.; Loncarek, J.; Sauer, M.; Schnermann, M. J. Cyanine Conformational Restraint in the Far-Red Range. *J. Am. Chem. Soc.* **2017**, *139*, 12406−12409.
(51) Matikonda, S. S.; Hammersley, G.; Kumari, N.; Grabenhorst, L.; Glembockyte, V.; Tinnefeld, P.; Ivanic, J.; Levitus, M.; Schnermann, M. J. Impact of Cyanine Conformational Restraint in the Near-Infrared Range. *J. Org. Chem.* **2020**, *85*, 5907−5915.
(52) Chung, H. S.; Eaton, W. A. Protein folding transition path times from single molecule FRET. *Curr. Opin. Struct. Biol.* **2018**, *48*, 30−39.
(53) Wu, Y.; Tilley, R. D.; Gooding, J. J. Challenges and Solutions in Developing Ultrasensitive Biosensors. *J. Am. Chem. Soc.* **2019**, *141*, 1162−1170.
(54) Zang, F.; Su, Z.; Zhou, L.; Konduru, K.; Kaplan, G.; Chou, S. Y. Ultrasensitive Ebola Virus Antigen Sensing via 3D Nanoantenna Arrays. *Adv. Mater.* **2019**, *31*, 1902331.
(55) Hrabak, J.; Chudackova, E.; Papagiannitsis, C. C. Detection of carbapenemases in Enterobacteriaceae: a challenge for diagnostic microbiological laboratories. *Clin. Microbiol. Infect.* **2014**, *20*, 839−853.
(56) Poirel, L.; Héritier, C.; Tolün, V.; Nordmann, P. Emergence of oxacillinase-mediated resistance to imipenem in Klebsiella pneumoniae. *Antimicrob. Agents Chemother.* **2004**, *48*, 15−22.
(57) Thacker, V. V.; Herrmann, L. O.; Sigle, D. O.; Zhang, T.; Liedl, T.; Baumberg, J. J.; Keyser, U. F. DNA origami based assembly of gold nanoparticle dimers for surface-enhanced Raman scattering. *Nat. Commun.* **2014**, *5*, 3448.
(58) Kuzyk, A.; Schreiber, R.; Fan, Z.; Pardatscher, G.; Roller, E.-M.; Högele, A.; Simmel, F. C.; Govorov, A. O.; Liedl, T. DNA-based self-assembly of chiral plasmonic nanostructures with tailored optical response. *Nature* **2012**, *483*, 311−314.
(59) Kuzyk, A.; Jungmann, R.; Acuna, G. P.; Liu, N. DNA Origami Route for Nanophotonics. *ACS Photonics* **2018**, *5*, 1151−1163.
(60) Kuzyk, A.; Schreiber, R.; Zhang, H.; Govorov, A. O.; Liedl, T.; Liu, N. Reconfigurable 3D plasmonic metamolecules. *Nat. Mater.* **2014**, *13*, 862−866.
(61) Prinz, J.; Schreiber, B.; Olejko, L.; Oertel, J.; Rackwitz, J.; Keller, A.; Bald, I. DNA Origami Substrates for Highly Sensitive Surface-Enhanced Raman Scattering. *J. Phys. Chem. Lett.* **2013**, *4*, 4140−4145.
(62) Rissin, D. M.; Kan, C. W.; Campbell, T. G.; Howes, S. C.; Fournier, D. R.; Song, L.; Piech, T.; Patel, P. P.; Chang, L.; Rivnak, A. J.; Ferrell, E. P.; Randall, J. D.; Provuncher, G. K.; Walt, D. R.; Duffy, D. C. Single-molecule enzyme-linked immunosorbent assay detects serum proteins at subfemtomolar concentrations. *Nat. Biotechnol.* **2010**, *28*, 595−599.

https://doi.org/10.1021/acs.accounts.1c00307
Acc. Chem. Res. 2021, 54, 3338−3348

(63) Ranallo, S.; Rossetti, M.; Plaxco, K. W.; Vallée-Bélisle, A.; Ricci, F. A Modular, DNA-Based Beacon for Single-Step Fluorescence Detection of Antibodies and Other Proteins. *Angew. Chem., Int. Ed.* **2015**, *54*, 13214−13218.
(64) Peng, S.; Wang, W.; Chen, C. Breaking the Concentration Barrier for Single-Molecule Fluorescence Measurements. *Chem. - Eur. J.* **2018**, *24*, 1002−1009.
(65) Chikkaraddy, R.; de Nijs, B.; Benz, F.; Barrow, S. J.; Scherman, O. A.; Rosta, E.; Demetriadou, A.; Fox, P.; Hess, O.; Baumberg, J. J. Single-molecule strong coupling at room temperature in plasmonic nanocavities. *Nature* **2016**, *535*, 127−130.
(66) Bohlen, J.; Cuartero-González, Á.; Pibiri, E.; Ruhlandt, D.; Fernández-Domínguez, A. I.; Tinnefeld, P.; Acuna, G. P. Plasmon-assisted Förster resonance energy transfer at the single-molecule level in the moderate quenching regime. *Nanoscale* **2019**, *11*, 7674−7681.

https://doi.org/10.1021/acs.accounts.1c00307
Acc. Chem. Res. 2021, 54, 3338−3348